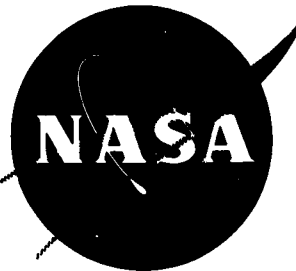


**NASA TECHNICAL
MEMORANDUM**



NASA TM X- 52192

NASA TM X- 52192

FACILITY FORM 602

N66-22937
(ACCESSION NUMBER)

13
(PAGES)

TMX-52192
(NASA CR OR TMX OR AD NUMBER)

(THRU)

1
(CODE)

33
(CATEGORY)

**RADIANT ENERGY TRANSPORT WITHIN
CRYOGENIC CONDENSATES**

by Dudley G. McConnell
Lewis Research Center
Cleveland, Ohio

GPO PRICE \$ _____

CFSTI PRICE(S) \$ _____

Hard copy (HC) 1.00

Microfiche (MF) .50

653 July 65

TECHNICAL PAPER proposed for presentation at
Annual Meeting and Equipment Exposition of the
Institute of Environmental Sciences
San Diego, California, April 11-13, 1966

RADIANT ENERGY TRANSPORT WITHIN CRYOGENIC CONDENSATES

by Dudley G. McConnell

Lewis Research Center
Cleveland, Ohio

TECHNICAL PAPER proposed for presentation at

Annual Meeting and Equipment Exposition of the
Institute of Environmental Sciences
San Diego, California, April 11-13, 1966

NATIONAL AERONAUTICS AND SPACE ADMINISTRATION

RADIANT ENERGY TRANSPORT WITHIN CRYOGENIC CONDENSATES

By: Dudley G. McConnell, Lewis Research Center



Dudley G. McConnell

Dr. McConnell received his B.M.E. degree from the City College of New York in 1957, at which time he joined the Special Projects Branch of the Lewis Laboratory. This branch was engaged in research into aerodynamic heating using free flight test models. Following receipt of his M.S. degree from Case Institute in 1959, Dr. McConnell participated in the design of the Lewis Space Environment Simulator and in developing techniques for accelerating particles in connection with micro-meteoritic impaction. In 1961, he began his dissertation researches into aerodynamic ablation for which he received his Ph.D. also from Case Institute in June of 1964. Dr. McConnell is currently a member of the Environmental Physics Section of NASA Lewis, where he is actively engaged in research in the thermodynamics of fluids and solids. Dr. McConnell is a member of Pi Tau Sigma, Sigma Xi, AIAA, and ASME.

ABSTRACT

A previous paper [1] presented an approximate analytical treatment of this problem. That treatment resulted in an expression for the apparent absorptance of the condensate that compared well with experimental data reported elsewhere. The expression showed that under certain specified conditions, the presence of a condensate could alter the heat transported to a surface significantly, when compared with the heat transported in the absence of a condensate. In obtaining a closed form solution, however, assumptions were made that might have had the effect of limiting the solution.

The present paper refines and extends the earlier analysis by:

- (1) allowing for an explicitly varying condensate depth
- (2) considering a range of substrate temperatures
- (3) treating emission from the condensate more precisely

In addition, a variety of boundary conditions have been imposed at the condensate-substrate interface in order to extend the applicability of the analysis.

The results to date indicate that the previous assumptions did not invalidate the earlier analysis for the broader class of problems considered here. Even at a substrate temperature of 250° K, the rate of sublimation from the condensate was so small that the variable condensate depth had a negligible effect upon the temperature distribution, as also did the emission. The effect of higher substrate temperature was to increase the heat loss coefficient \bar{h} of the condensate. Problems with other boundary conditions are being investigated.

INTRODUCTION

A previous paper [1] presented an approximate analytical treatment of the transport of thermal energy in an H₂O deposit exposed to thermal radiation in a vacuum. The deposit (frost) was assumed to have grown on the exterior surface of a cryogenic fuel tank. The analysis showed that the presence of an H₂O deposit could increase the heat transported through a reflective surface by as much as a factor of eight over the value transported through the bare surface. To achieve this closed form solution, however, two principle assumptions were made: (1) the change in deposit thickness due to sublimation was assumed to be negligible, so that the differential equation of heating showed no explicit dependence upon the rate of sublimation, and (2) the radiant energy emitted by the frost was combined with the heat lost by sublimation and both were treated in the boundary conditions. The purpose of the present paper is to refine the analysis by removing these assumptions, and further, to apply the refined analysis to the case of cryodeposits formed upon shadow shields and within multifoil insulation systems.

ANALYSIS

The situation to be analyzed is presented in figure 1. Thermal radiation is incident upon a nonopaque solid, the cryodeposit, which covers the exterior metallic surface of a cryogenic reservoir. Of the radiant energy incident upon the frost, certain portions will be

- (1) Reflected to space at the vacuum-frost interface
- (2) Consumed in sublimation of the frost
- (3) Absorbed in the frost raising the frost temperature
- (4) Absorbed in the frost and conducted to the reservoir
- (5) Absorbed in the frost and reradiated to space
- (6) Transmitted through the frost directly to the metallic substrate

Of the radiation transmitted through the frost di-

E-3423

rectly to the substrate, a portion will be reflected back to the frost again as determined by the reflectance at the frost-metal interface. By considering the energy balance for a differential volume element (shown in fig. 1) the following heat transfer equation is obtained:

$$\rho c_p \left(\frac{\partial T}{\partial t} \right) = k \left(\frac{\partial^2 T}{\partial y^2} \right) + (1 - \rho_{12}) W_{inc} \kappa_a \times \left\{ e^{-\kappa_a [H-s-y]} + \rho_{23} e^{-\kappa_a [H-s+y]} \right\} - \kappa_e \sigma (T^4 - T_c^4) \quad (1)$$

where κ_a is the absorption coefficient averaged over a spectral region of interest (the "box" approximation of [2]) and W_{inc} is the incident radiant energy in that spectral region. This definition of κ_a and W_{inc} is well suited to materials that are absorbent over limited spectral regions. In such cases, the contribution of each absorption band would simply be added. The absorption coefficient, κ_e , is also averaged, but over the spectral region of emission. In this analysis, κ_a , κ_e , and all other physico-chemical properties of the deposit are considered to be known. Symbols are defined in the appendix and physical properties used in the calculations are presented in table I.

TABLE I. - PHYSICAL PROPERTIES OF WATER CRYODEPOSIT

Property	Value
Density of ice ¹	0.917 g/cu cm
Heat of sublimation ¹	3050 J/g
Specific heat ²	0.697 J/(g)(°K)
Thermal conductivity ³	0.078 J/(cm)(sec)(°K)
Absorption coefficient for solar radiation ⁴	0.0305/μ
Absorption coefficient for 290° K blackbody ⁴	0.1578/μ
Absorption coefficient for 77° K blackbody ⁴	0.0640/μ
Emission for 250° K case	0.1578/μ

¹Ref. 3.

²Ref. 4

³Ref. 5

⁴Ref. 6

In physical terms, the boundary conditions on the solution of the problem are:

(1) The substrate temperature is constant and equal to T_c

(2) The frost may lose heat and mass at the vacuum surface as a result of sublimation.

(3) The frost is in a quiescent steady-state condition at a definite thickness H and definite temperature T_c prior to the incidence of thermal and radiation.

The analytical statement of these conditions is:

$$\begin{aligned} \text{at } y = 0 & \quad T = T_c \\ \text{at } y = H - s & \quad -k \left(\frac{\partial T}{\partial y} \right) = \dot{m} L_s \\ \text{at } t = 0 & \quad T = T_c \end{aligned}$$

Equation (1) is nondimensionalized by means of the following substitutions

$$\theta \equiv \frac{T - T_c}{T_c}; \quad \xi = \kappa_a [(H - s) - y]; \quad \tau = \frac{k \kappa_a^2 t}{\rho c_p};$$

$$\sigma_s(t) \equiv \kappa_a s(t); \quad h \equiv \kappa_a H$$

Thus, θ is the temperature rise scaled by the substrate temperature, ξ is the optical depth of the frost, and τ is the Fourier number of classical conduction heat transfer. The quantities σ_s and h are introduced for convenience. In terms of these new variables, the heat transfer equation is

$$\frac{\partial \theta}{\partial \tau} \equiv \dot{\sigma}_s \left(\frac{\partial \theta}{\partial \xi} \right) = \left(\frac{\partial^2 \theta}{\partial \xi^2} \right) + Q \left\{ e^{-\xi} + \rho_{23} e^{-[2(h-\sigma_s)-\xi]} \right\} - Q' \theta \quad (1a)$$

where

$$Q \equiv \frac{(1 - \rho_{12}) W_{inc}}{k \kappa_a T_c}; \quad Q' \equiv \frac{4 \kappa_e \sigma T_c^4}{k \kappa_a^2 T_c}$$

In order to show the extensions involved in the present analysis, the present heat transfer equation (1a) is compared with the equivalent equation solved in [1]. In terms of the present symbols that equation is

$$\frac{\partial \theta}{\partial \tau} = \left(\frac{\partial^2 \theta}{\partial \xi^2} \right) + Q \left[e^{-\xi} + \rho_{23} e^{-(2h-\xi)} \right]$$

This last equation is obtainable from (1a) if:

(1) The contribution of the emission term Q' is not included in the equation.

(2) $\sigma_s \ll h$

(3) $\dot{\sigma}_s \left(\frac{\partial \theta}{\partial \xi} \right) \ll \left(\frac{\partial \theta}{\partial \tau} \right)$

These conditions were assumed in [1]; however, these assumptions are not made in the present analysis.

The partial differential equation that is solved in the present analysis is

$$\frac{\partial \psi}{\partial \tau} - \dot{\sigma}_s \left(\frac{\partial \psi}{\partial \xi} \right) = \left(\frac{\partial^2 \psi}{\partial \xi^2} \right) + \left\{ e^{-\xi} + \rho_{23} e^{-[2(h-\sigma_s)-\xi]} \right\} - Q' \psi \quad (2)$$

where $\psi \equiv (\theta/Q)$ is introduced for convenience. As shown in detail in [1], the boundary conditions may be linearized to result in the following:

$$\begin{aligned} \text{at } \xi = 0 \quad \frac{\partial \psi}{\partial \xi} - \bar{h}\psi &= 0 \quad \bar{h} \equiv \frac{\left[\frac{\partial(\bar{m}L_s)}{\partial T} \right]_{T=T_c} T_c}{k\kappa_a T_c} \\ \text{at } \xi = h - \sigma_s \quad \psi &= 0 \\ \text{at } \tau = 0 \quad \psi &= 0 \end{aligned}$$

Finally, there is a subsidiary relation for $\dot{\sigma}_s$

$$\dot{\sigma}_s = \left(\frac{\kappa_a T_c}{\rho L_s} \right) \left[\left(\frac{\partial \bar{m}L_s}{\partial T} \right)_{T=T_c} \right] \theta_{\xi=0}$$

Several analytical solutions of (2) were investigated in a cursory fashion. Notable among these was a solution in terms of a transformation first suggested by Paterson [7] and more recently by Sneddon [8]. By means of the transformation

$$u \equiv \psi e^{Q'\tau}$$

equation (2) becomes

$$\frac{\partial u}{\partial \tau} - \dot{\sigma}_s \left(\frac{\partial u}{\partial \xi} \right) = \frac{\partial^2 u}{\partial \xi^2} + e^{Q'\tau} \left\{ e^{-\xi} + \rho_{23} e^{-[2(h-\sigma_s)-\xi]} \right\}$$

As $Q' \approx 0[10^{-5}]$, the solution to this equation would be expected to be very similar to that presented in [1] were it not for the convective term, $\dot{\sigma}_s \left(\frac{\partial u}{\partial \xi} \right)$, whose contribution could be significant.

No exact solution was found for the equation containing the convective term; therefore, a numerical solution was sought. In this way, a measure of the contribution of each term could be obtained.

Figure 2 presents the spatial distribution of the dimensionless temperature rise through a water frost on a 250° K substrate. The physical properties of the frost are listed in table I. The reason for this choice of substrate temperature will be clarified subsequently. The time at which steady-state was achieved was arbitrarily defined as that time after which there was no change in the third significant figure of ψ . In figure 2, the abscissa is $\xi/(h - \sigma_s)$; however, for all cases considered, it was found that $\sigma_s < 10^{-2} h$.

The complete energy flux to the reservoir is given by

$$Q_{\text{tot}} = (1 - \rho_{23})(W_{\text{inc}} - W'_{\text{inc}}) + \alpha_{\text{tot}} W'_{\text{inc}} (1 - \rho_{12})$$

In a particular case, the dominant absorption term will depend upon the spectral properties of the deposit (i.e., κ as a function of wavelength). The expression for α_{tot} is

$$\alpha_{\text{tot}} = \left(\frac{\partial \psi}{\partial \xi} \right)_{\xi=h-\sigma_s} + (1 - \rho_{23}) e^{-(h-\sigma_s)}$$

Thus, the curves for α_{tot} , presented in figure 3, give the heat flux to the substrate by conduction from the frost and radiant transmission through the frost in the spectral region appropriate for W'_{inc} . These curves, which were first presented in [9], give the heat transfer at steady state as defined previously. In the present paper, a rather high value of substrate temperature (250° K) was chosen in order to assess the effect of an appreciable mass-transfer rate. Even for this case, $\sigma_s \ll h$. As an example for $h = 0.125$ with the deposit at 250° K subjected to 290° K blackbody radiation, $\sigma_s = 0.15 \times 10^{-7}$ at steady-state. Thus, the assumption $\sigma_s \ll h$ is valid for this case. Recall that [1], based upon that assumption, did achieve a truly steady-state solution. Therefore, the results presented here tend to confirm the results presented in [1], and further, the steady-state results as here defined are equivalent to the steady-state results of [1]. For the H₂O deposit considered here, the wavelength region of interest was taken to be 2 to 20 microns for absorption and 2 to 100 microns for emission from a substrate whose temperature ranged from 20° to 250° K. The spectral regions were chosen to include the principle absorption bands of the deposit. A temperature of 250° K could be obtained by the bulkhead of a spacecraft on the night side of an Earth orbit or by an interior surface of a shadow shield array. Thus, these findings indicate that a deposit, once formed, could remain stable on such surfaces.

The results of a more complete analysis tend to confirm the validity of the assumptions made in an earlier analysis, namely, that $\sigma_s \ll h$, and that the effects of Q' and $\dot{\sigma}_s \frac{\partial \psi}{\partial \xi}$ are negligible. Several applications of cryodeposits now will be investigated.

APPLICATIONS

In the case of bare surface reflectance shielding, the effect of a cryodeposit is shown in figure 3. From the analysis of [1] and figure 3, the total heat transport due to incident energy in the range W_{inc} decreases as $1/h$ for $h > 1.0$ and $h \gg 1.0$. On this basis, [9] suggested that a deposit could be used to reduce heat transport to a surface that had been degraded. To accomplish this, the minimum deposit optical thickness is given by the condition that

$$(1 - \rho_{12}) \alpha_{\text{tot}} < 1 - \rho_{23}$$

Bare surfaces of cryoreservoirs, however, are rarely, if ever, exposed to direct solar radiation. Most often, at least one additional surface exists. Depending upon the temperature of that surface, the radiation it emits could be in just that spectral region for which the frost is most absorbent (e.g., 2 to 20 μ in the case of H₂O). Specific examples have been calculated for the configuration of shields and cryodeposits shown in figure 4. The steady-state thermal energy flux through a two shield array is obtained from the simultaneous solution of the following equations:

$$\alpha W_{\text{inc}} - \epsilon_1 \sigma T_1^4 = \epsilon_{12} F_{12} \sigma (T_1^4 - T_2^4) + \epsilon_1 (1 - F_{12}) \sigma T_1^4$$

$$E_{12}F_{12}\sigma(T_1^4 - T_2^4) - \epsilon_2(1 - F_{12})\sigma T_2^4 \\ = E_{2R}F_{2R}\sigma(T_2^4 - T_R^4) + \epsilon_2(1 - F_{2R})\sigma T_2^4$$

where

$$E_{ij} = \frac{1}{\frac{1}{\epsilon_i} + \frac{1}{\epsilon_j} - 1}$$

and where α and W_{inc} refer to the complete solar spectrum. The present calculations are based upon $T_R = 20^\circ \text{K}$, $F_{12} = 0.382$, and $\epsilon = 0.045$ for the bare shield surface (e.g., aluminum foil). It is further assumed that the surfaces with deposits have emittances of 0.090. As shown in figure 3, this emittance would correspond to a frost thickness of less than 3μ for $\kappa_a = 0.1578$ per μ . The resultant heat fluxes to the cryoreservoir are shown in figure 4 for each configuration. In both cryodeposit cases, the heat flux is increased by over 30 percent due to the presence of the deposit. It is acknowledged that the figures quoted are based upon a steady-state calculation. Nevertheless, the temperature attained by the inner shield and the temperature of the reservoir are such that a deposit, once formed, can remain stable.

The effect of the boundary condition of constant-reservoir temperature was investigated to determine the applicability of the present analysis (i.e., the solution of eq. (2)) to the shielding problems. As an extreme, the rate of sublimation was calculated for the case in which the inner frost surface was insulated against conduction heat transfer. Even in this case, a steady-state temperature distribution was obtained while $\alpha_s \ll h$. Thus, the calculations are valid for the case of shadow shields.

P. J. Perkins, of NASA Lewis, suggests that multilayer insulation be vacuum sealed and filled with a readily condensable gas such as CO_2 in order to provide a cryopumped vacuum within the insulation while in the Earth's atmosphere. In order to investigate the effect of the condensate upon the effectiveness of the system, a simplified multilayer insulator was investigated. It was assumed that five shielding layers separated by vacuum spacing were used to shield a fuel tank. In the steady-state the heat flux to the reservoir is given by

$$W_{net} = \alpha W_{inc} - \epsilon_1 \sigma T_1^4$$

Again, for bare surfaces $\epsilon = 0.045$; for frost covered surfaces, $\epsilon = 0.090$. Since W_{net} is also the net flux between neighboring foils, there results five equations for five unknown foil temperatures (T_R is presumed known). For the case of bare shields, $W_{net} = 1.99 \times 10^{-3}$ watts per square centimeter and for the case where a condensate forms on the reservoir and the innermost shield, $W_{net} = 2.18 \times 10^{-3}$ watts per square centimeter, a 10-percent increase in the boiloff heat flux. The model considered here does not allow for spacer conductance or gas conductance between shields whose temperatures would preclude condensation. Both of these conductances could easily increase the heat flux by more than 10 percent. Consequently, it does

not appear that the condensate would adversely influence the effectiveness of a multilayer insulation system.

In conclusion, a numerical solution of the complete heat balance equation has substantiated an earlier preliminary analysis of heat transport in a nonopaque frost layer. In particular, sublimation was found to be sufficiently small for all cases considered such that $\alpha_s \ll h$. Thus, it was concluded that the previous analysis was adequate. With this in mind, the results of [9] were reviewed and extended to the case of multilayer insulators. It was found that the effectiveness of the multilayer insulation system probably would not be adversely affected by the presence of a cryogenic condensate.

APPENDIX - SYMBOLS

c_p	specific heat of deposit
E_{ij}	radiant exchange factor between parallel plane surface i, j
F_{ij}	configuration factor for parallel plane circular surfaces ij
H	initial frost thickness
h	initial frost optical thickness $\kappa_a H$
\bar{h}	linearized heat loss coefficient
k	thermal conductivity of deposit
L_s	heat of sublimation of deposit
\dot{m}	rate of deposit mass loss due to sublimation
Q	dimensionless incident radiant energy
Q_{tot}	complete energy flux to reservoir
Q'	dimensionless emitted radiant energy
s	sublimed deposit depth
\dot{s}	rate of sublimation, real time
T	temperature
T_c	temperature of substrate
T_R	reservoir temperature
t	time
W_{inc}	total incident radiant energy
W'_{inc}	radiant energy in spectral region for which frost absorbs
y	spatial variable
α	absorptance
α_{tot}	total dimensionless heat flux
ϵ	emittance

θ	dimensionless temperature rise
κ_a	absorption coefficient, averaged over spectral region of interest
	$\kappa_a = \int_{\lambda_1}^{\lambda_2} \kappa_\lambda d\lambda / (\lambda_2 - \lambda_1).$ See [2], the "box" approximation.
κ_e	absorption coefficient, average over spectral region appropriate to the emitted energy
λ	wavelength
ξ	dimensionless spatial variable
ρ	density of deposit
ρ_{12}	reflectance at exterior interface
ρ_{23}	reflectance at interior interface
σ	Stefan-Boltzmann constant
σ_s	optical depth loss due to sublimation
$\dot{\sigma}_s$	rate of sublimation, transformed time
τ	transformed time (Fourier number)
ψ	dependent variable for dimensionless temperature rise

9. McConnell, Dudley G.: Effects of Cryodeposits on Space-Craft Thermal Control Systems. Paper Presented at Nat. Conf. on Space Maintenance and Extravehicular Activities, USAF and Martin Co., Orlando, Fla., Mar. 1-3, 1966.

REFERENCES

1. McConnell, Dudley G.: Absorptance of Thermal Radiation by Cryodeposit Layers. Paper Presented at Cryogenic Eng. Conf., Houston, Texas, Aug. 23-25, 1965.
2. Penner, S. S.: Quantitative Molecular Spectroscopy and Gas Emissivities. Addison-Wesley Publ. Co., Reading, Mass., 1959.
3. Gray, Dwight E., ed.: American Institute of Physics Handbook. Second ed., McGraw-Hill Book Co., Inc., New York, N.Y., 1963.
4. Washburn, E. W., ed.: International Critical Tables of Numerical Data, Physics, Chemistry and Technology. McGraw-Hill Book Co., Inc., New York, N.Y., 1926-1930.
5. Ratcliffe, E. H., Phil Mag. 7, July, 1962. (1197-1203).
6. Kislovskii, L. D., Optics and Spectroscopy 7, Sept. 1959 (201-206).
7. Paterson, S.: Conduction of Heat in a Medium Generating Heat. Phil. Mag. 32, No. 214, Nov. 1941 (384-392).
8. Sneddon, Ian N.: Fourier Transforms. McGraw-Hill Book Co., Inc., New York, N.Y., 1951.

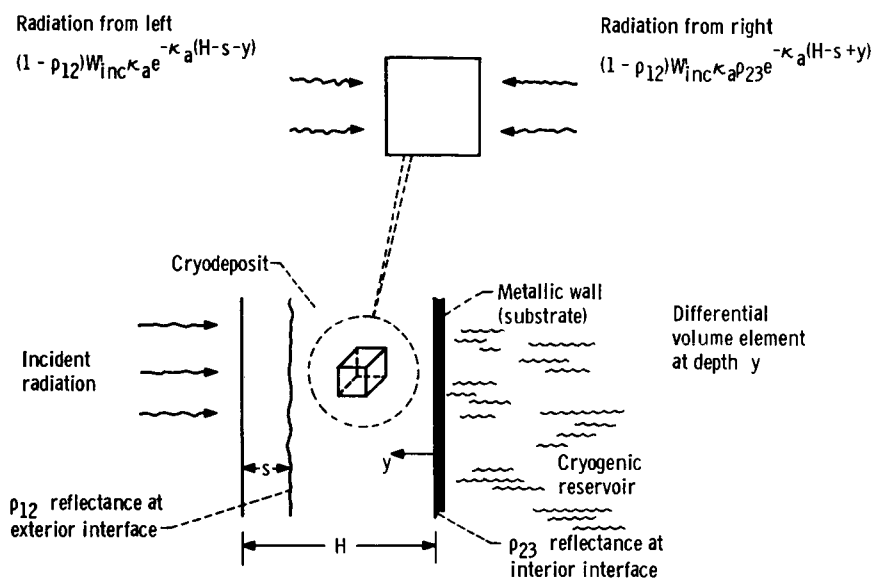


Figure 1. - Cryodeposit and substrate complex.

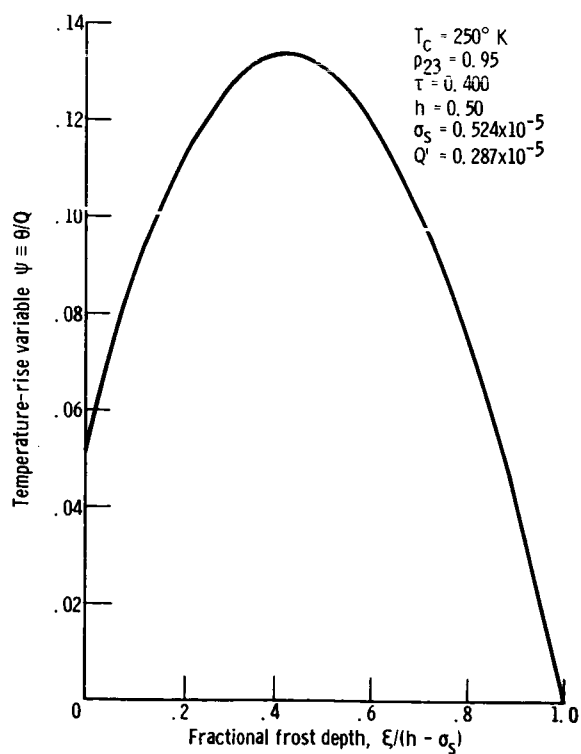


Fig. 2. - Steady-state distribution of dimensionless temperature rise.

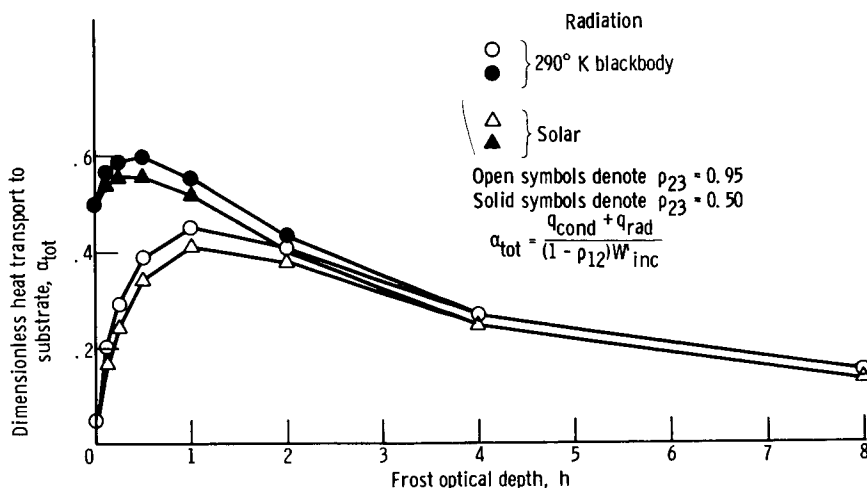


Fig. 3. - Total dimensionless heat transport through a 250° K substrate for solar and 290° K blackbody radiation.

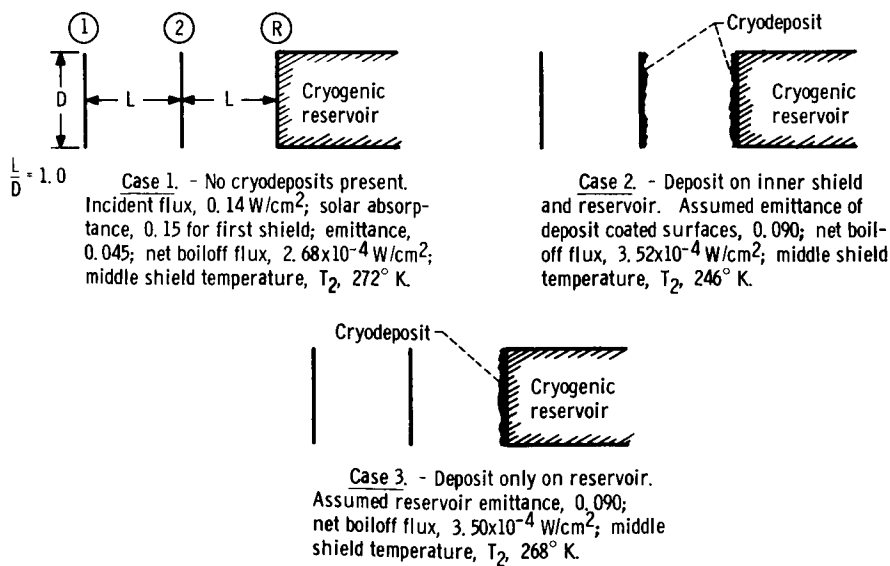


Fig. 4. - Effect of cryodeposition on shadow shields.